NASA
Technical
Paper
1663

February 1982

High-Speed Laser Anemometer System for Intrarotor Flow Mapping in Turbomachinery

J. Anthony Powell,
Anthony J. Strazisar,
and Richard G. Seasholtz

NASA

NASA
Technical
Paper
1663

1982

High-Speed Laser Anemometer System for Intrarotor Flow Mapping in Turbomachinery

J. Anthony Powell,
Anthony J. Strazisar,
and Richard G. Seasholtz
Lewis Research Center
Cleveland, Ohio

National Aeronautics
and Space Administration

Scientific and Technical
Information Branch

Summary

Since turbomachinery research facilities often consume large amounts of energy, there is an increasing need that experiments be performed quickly. A fringe-type laser anemometer with innovative features directed toward answering this need is described. These features include (1) a rapid and efficient data acquisition process, (2) a detailed real-time graphic display of the data being accumulated, and (3) input laser beam positioning that allows greater optical access to the intrarotor region. Details of both system hardware and sofeware are described. Results are presented that demonstrate the anemometer's capability in flow mapping within a transonic axial-flow compressor rotor. Typically, a velocity profile, derived from 30 000 measurements along 1000 sequential circumferential positions covering 20 blade passages, can be obtained in 30 seconds. The use of fluorescent seed particles allows flow measurements near the rotor hub and the casing window.

Introduction

To improve the understanding of flow phenomena in turbomachinery, and to verify flow models used in analysis, detailed measurements of the internal flow field of the rotating components are needed. Increasingly, laser anemometry (ref. 1) is being used to answer this need. In the past several types of laser anemometers (LA) have been applied to turbomachinery. Among these are the fringe-type anemometer (sometimes called a laser Doppler velocimeter; refs. 2 and 3) and the time-of-flight anemometer (refs. 4 to 6).

Since turbomachinery research facilities often consume large amounts of energy, there is an additional need that flow measurements be made as quickly as possible. In each of the systems described in references 2 and 4 to 6, the laser was time-gated so that velocity measurements were accepted only during a small fraction of each revolution of the rotor. The reason for this is as follows: The probe volume, fixed at some axial and radial position, sweeps out a circumferential path within the rotating blade row. In each case the circumferential path in a given blade passage was divided into a fixed number of line segments, and the velocity for each segment was determined, one segment at a time. This was accomplished by time-gating the system so that measurements were made only when the desired line segment was in the field of view. In the system of references 5 and 6, measurements from corresponding segments in successive blade passages were averaged in order to speed up the data taking rate. However, in all of the time-gated systems, the data acquisition process is very wasteful of facility run time. In the system described in reference 3, data are continuously collected from a circumferential path covering two blade passages. The individual measurements are then presented as marks on an oscilloscope display such that the veritical position of each mark represents the velocity and the horizontal position represents the circumferential location of the measurement. Measurements are recorded by photographing the oscilloscope display. This approach does not lend itself to efficient data recording or later data analysis.

Recent applications of laser anemometers to turbomachinery (refs. 7 to 9) use a more efficient data collection process. In these systems velocity measurements are accepted randomly over a range of rotor angles, and the corresponding angle is determined for each measurement. In reference 7 an optical encoder, attached to the shaft of the turbomachine, is used. Marker pulses, provided by the encoder, and the time between measurements allow the calculation of the rotor angle for each velocity measurement. In refences 8 and 9 the rotor angle corresponding to each velocity measurement is generated electronically, based on one-per-revolution and/or once-per-blade signals derived from the spinning rotor.

This paper is a more detailed description of the system of reference 9, wherein velocity measurements, at any given time, are accepted from any of 1000 line segments along the circumferential path. Each velocity measurement is tagged with the location of the line segment in which it occurred and the resulting data sorted with a minicomputer. Adding to the efficiency of the anemometer is a real-time graphic display that allows the evaluation of data being accumulated. The anemometer also makes use of techniques that minimize the portion of the intrarotor region that cannot be mapped because of shadowing due to blade twist.

The anemometer was used to map the intrarotor region of a transonic axial-flow compressor rotor. The rotor contained 52 blades and had an overall diameter of 50.8 centimeters. It was operated at a maximum speed of about 16 000 rpm. Sufficient results are presented to demonstrate the capability of the anemometer. The 20 blade passages that were mapped represent 40 percent of a complete circumference for this particular rotor. This application is discussed in detail in another paper (ref. 10).

A 16-millimeter-film supplement, "High-Speed Laser Anemometer for Intrarotor Flow Mapping in Turbomachinery," is available that explains and illustrates the anemometer's operation. Information on obtaining this film is included at the end of this report.

Description of System Hardware

Brief Overall Description

Figure 1 shows the basic optical components of the LA. It is a fringe type, on-axis, backscattering system that uses the 514.5 nanometer (green) line of an argon-ion laser. In a fringe type LA, the flow velocity is determined by measuring the transit time required for a seed particle to traverse several fringes of known spacing. The fringes occur at the intersection (called the probe volume) of two laser beams derived from the same laser by means of the beam splitter. The particular velocity component being measured lies in the plane of the two beams and is perpendicular to the bisector of the two beam axes. The component is selected by rotating the splitter to the required angle. Optical access to within the rotor-blade row is made through a window in the casing around the rotor along a path that is approximately radial. The motorized-goniometer mirror mount, shown in the figure, allows the direction of the converging beams to be adjusted to minimize shadowing due to the twisted rotor blades. This ability to position the bisector of the input laser beams in an off-radial direction also allows, at least in principle (ref. 10), the measurement of the radial component of velocity. Fluorescent seed particles coupled with an orange-pass optical filter in the receiving optics reduce detection of unwanted scattered light. This allows measurements near the rotor hub and casing window.

Figure 2 is a simplified block diagram of the complete laser anemometer system. Velocity measurements occur

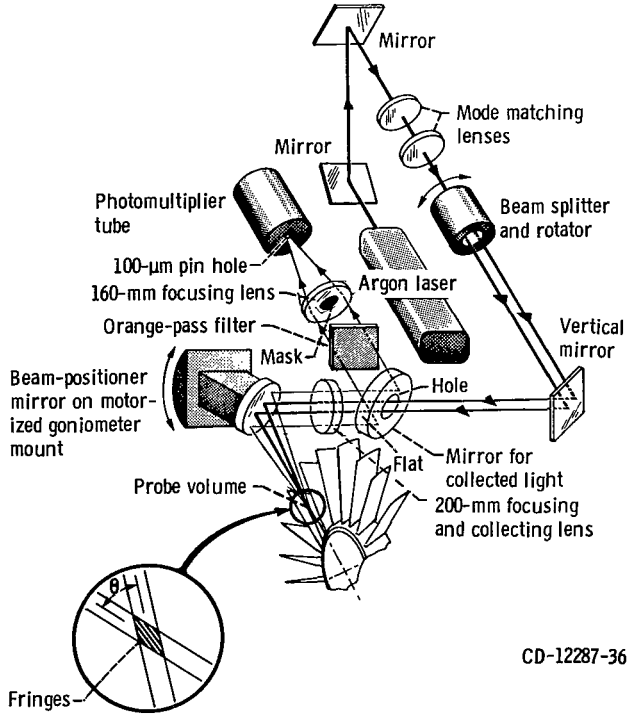

Figure 1. - Optical layout of anemometer.

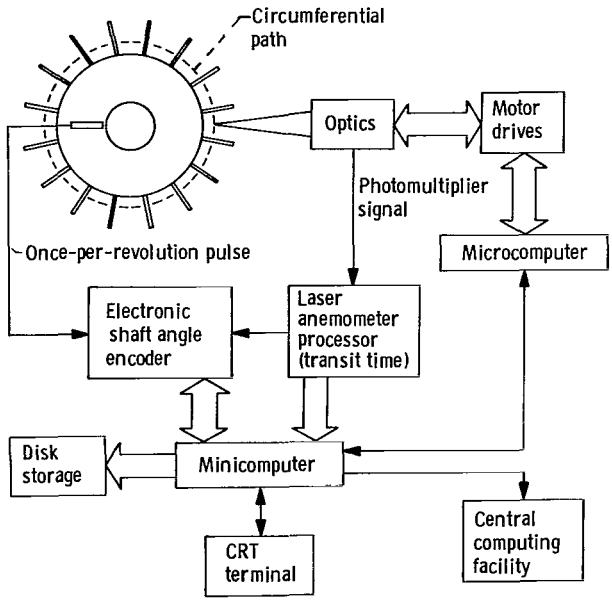

Figure 2. - Block diagram of complete anemometer.

randomly along the swept circumferential path since a measurement depends on the random passing of a seed particle through the proble volume. At any given time the system accepts measurements from any of 1000 sequential angular positions along this circumferential path. The position information for each velocity measurement is provided by an electronic shaft angle encoder that was developed for this system. When a measurement is obtained, the transit time between fringes and the rotor position are recorded and processed by the minicomputer. In this way velocity measurements are accumulated at random points along the circumferential path until a preset number of measurements is obtained. In most cases 30 000 measurements are accumulated, which results in an average of 30 measurements per angular position. The choice of the number of angular positions (1000) is influenced by the available computer memory. In this paper velocity measurements along a circumferential path covering up to 20 blade passages is called a velocity profile. A complete velocity map is obtained by determining these velocity profiles at a sequence of axial and radial positions. After each profile is obtained, the data are stored on a magnetic disk.

Overall control of the anemometer is maintained through a cathode ray tube (CRT, i.e., video) terminal. During each data run, a CRT display of the accumulated data is updated as often as every 5 seconds. The display contains (1) alphanumeric information on operating conditions, (2) a plot of the blade-to-blade average velocity profile, and (3) a histogram showing the distribution of measurements over the 1000 angular positions.

Optics

The anemometer uses the 514.5-nanometer line of an argon ion laser operating in the TEM_{00} mode at a power

level of 1.5 watts. The laser beam (see fig. 1) is turned through 180° (for compactness) before passing through two mode matching lenses. The function of these lenses will be discussed near the end of this section.

The optical path through the beam splitter is shown in figure 3. The splitter is rotated about the optical axis to select a particular velocity component. The two optical flats are coated to provide two equal-intensity beams and to minimize losses. This particular splitter configuration yields equal path lengths for the two beams and symmetrical placement of the two beams about the optical axis. The splitter flats are coated for S polarization, which means that the electric field vector of the incident laser beam must be perpendicular to the plane of incidence, that is, the plane containing the surface normal and the incident beam. A $\lambda/2$ (half-wavelength) retardation plate, placed in front of the splitter, rotates the normally vertical polarization of the laser beam to follow the splitter rotation. However, a characteristic of the $\lambda/2$ retardation plate is that it rotates the direction of polarization twice the angle through which it turns. So, the retardation plate is rotated at half the angle of the beam splitter.

Again referring to figure 1, after passing through the 200-millimeter focal length focusing lens (50-mm diam), the two beams are turned 90° by a mirror mounted on a motorized goniometer cradle. The angle θ between the two converging beams was determined to be 2.82° by projecting the beams on a wall at a distance of about 3 meters and measuring the distance to the wall and the separation of the projected spots. Because the spots were blurred, multiple measurements of the spot separation were made with the beam splitter set at different angles. The resulting standard deviation in θ from these measurements was 0.03°. With this θ and a wavelength of 514.5 nanometers, the fringe spacing is 10.4 micrometers.

Some of the light scattered from seed particles passing through the probe volume is collected and directed to a 100-micrometer-diameter pinhole in front of the photomultiplier tube. The focusing lens in front of the photomultiplier tube is 50 millimeters in diameter, with a focal length of 160 millimeters. The combination of the 160-and 200-millimeter focal lengths of the two focusing lenses yields a pin-hole image diameter of 125 micrometers at the probe volume. Actually, the beam waist diameter at the probe volume dictates the selection of image diameter, and hence the pin-hole diameter. The focusing lenses are commercially available cemented doublets corrected to obtain negligible spherical aberration (to third order) for an object-to-image ratio of infinity. A 25-millimeter-diameter mask over the central part of the 160-millimeter lens is used to reduce the effective length of the probe volume to about 2 millimeters.

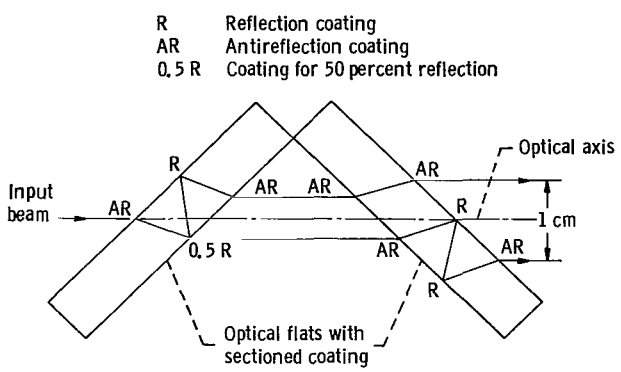

Figure 3. - Optical path through beam splitter.

The effective f-number of the optics for the collection of scattered light was reduced from the f/4 of the 200-millimeter focusing lens to about f/5 for several reasons. These reasons include the 25-millimeter mask and the reduced cross section of the goniometer mirror (50-mm diam) due to the 45° angle. Another reason is that the mirror (the one with a hole in the middle) had a flat ground on the edge. This flat was located so as to face the rotor in order to reduce the chance of mechanical interference with the rotor casing.

The reasons for the mode-matching lenses are as follows: With each mode-matching lens at the proper position, the beam waists will be at the probe volume; hence, the fringe planes will be parallel (ref. 11). Also, the waist diameter will be the proper diameter and this will maximize the laser power in the field of view of the photomultiplier tube. A waist diameter of 125 micrometers based on the $1/e^2$ intensity points, was selected because the LA processing electronics requires at least 10 fringes and the fringe spacing was 10.4 micrometers.

Although the approximate position of the mode-matching lenses can be calculated (ref. 11), their final position was found by trial and error. A procedure that the authors used is the following: Project the fringes on a wall with a microscope objective. Adjust the separation between the mode-matching lenses until about 12 fringes can be seen. Move the microscope-objective focus ±1 millimeter from the probe volume center along the beams' bisector and observe any change in the projected fringe spacing. Adjust the positions of the two mode-matching lenses along the laser beam axis, keeping their separation constant, until the projected fringe spacing remains the same as the microscope objective is moved. This step insures that the fringe planes are parallel.

All of the optics, including the laser, are located on a large horizontal x,y traversing table. With this table, the probe volume can be located at a particular axial and radial position within 0.05 millimeter over a range of 25 centimeter in either direction. The beam splitter can be rotated to within 0.01° over a 360° range. The direction of the input beams (i.e., the bisector of the two beams) can be oriented to within 0.01° using the goniometer-mounted mirror over a range of ±30° from horizontal.

System Computers and Electronics

To obtain efficient operation, a minicomputer is used to process the enormous amount of data generated and to

provide the required system control. The minicomputer, a 16-bit-word computer, has 32k (k = 1024) words of core memory and hardware floating-point multiply-divide capability. These features allow large tables of data to be stored and processed quickly. It also has dual cartridge-type magnetic disk storage, with each disk having a capacity of 1.25 million 16-bit words. The minicomputer terminal has a CRT display for presentation of both alphanumeric and graphic information. Also, the minicomputer is connected by phone lines to a large central computer, to which data are transmitted for both further processing and curve plotting.

A commercial, counter-type LA processor with a 500-megahertz clock processes the signal bursts from the photomutiplier tube. The processor measures the transit time of a seed particle across eight fringes. It performs several tests on each signal burst from a seed particle passing through the probe volume to help discriminate against noise and to insure measurement validity. One of these tests is the 5/8 comparison test where the transit times for five and eight fringes are compared. The ratio of these two times must be sufficiently close to the value of 5/8 to be accepted. Another test is a sequence check (ref. 12) such that during each signal burst, the high-pass filtered signal from the photomultiplier tube must alternately rise above a threshold level and fall below the zero level at each fringe in order to be accepted.

For each validated measurement the processor loads a digital representation of the transit time for the eight fringes into an output buffer register. Also, the electronic shaft angle encoder (to be described in the next section) is signaled, and the current rotor angular position is loaded into the encoder output buffer register. The processor also interrupts the minicomputer, which then records the transit time and the angular position. For the particular application described in this paper, measurement rates within a circumferential path being mapped were about 2500 measurements per second, and transit times were of the order of 50 nanoseconds per fringe across the fringe spacing of 10.4 micrometer.

In keeping with the design goal of efficient data taking, the motions required to position the probe volume and select the velocity component are controlled by the minicomputer. High-speed stepping motors provide the following four motions: the axial and the radial probe volume position (x-y traversing table), the beam splitter angle, and the input beam direction (goniometer cradle). An optical encoder attached to each motor shaft provides position feedback to each motor drive. The motor drives are of the accelerate-decelerate type (with regard to the output pulse train) and typically position the optics in about 1 second. Each motor has a "home" position to which it can be moved for remote position calibration.

An 8-bit-word microcomputer serves as the interface between the four motor drives and the minicomputer. The microcomputer and the motor drives are located in the test cell and the minicomputer is located in a control room. To minimize noise pickup in transmitting data between these two computers, a standard 20-milliampere asynchronous current loop is used.

Electronic Shaft Angle Encoder

The electronic shaft angle encoder was developed for the anemometer to simplify the task of tagging each velocity measurement with the proper angular position. The following procedure could have been used to determine the angular position of each velocity measurement: At each velocity measurement the time of occurrence is recorded relative to some reference position on the rotor. Because of rotor speed drift, the time of each complete revolution is also recorded. Now, each angular position can be calculated based on these recorded times. This calculation would have to be performed in real time for each velocity measurement. Otherwise, the "time of occurrence" and "time of revolution" would have to be stored with each velocity measurement.

Another approach to determining angular position is to use an optical encoder. This approach was not applicable for this system because the rotor speed exceeded the range of commercial encoders and because mechanical access to the rotor shaft was not practical.

The electronic encoder that was developed is shown in figure 4. It produces the current angular position independent of rotor speed with the only required input being an accurate once-per-revolution (OPR) pulse. Although the encoder involves the use of the minicomputer, a commercial stand-alone version is now available with the required computational logic circuits included. At this point it should be mentioned that the encoder has applications beyond the anemometer described in this paper. Any application requiring the knowledge of the instantaneous angular position of a high-speed rotor could make use of the encoder.

The encoded angular position of the rotor is produced by the counter that is clocked by the frequency synthesizer. The synthesizer frequency is adjusted as necessary by the minicomputer so that the number of

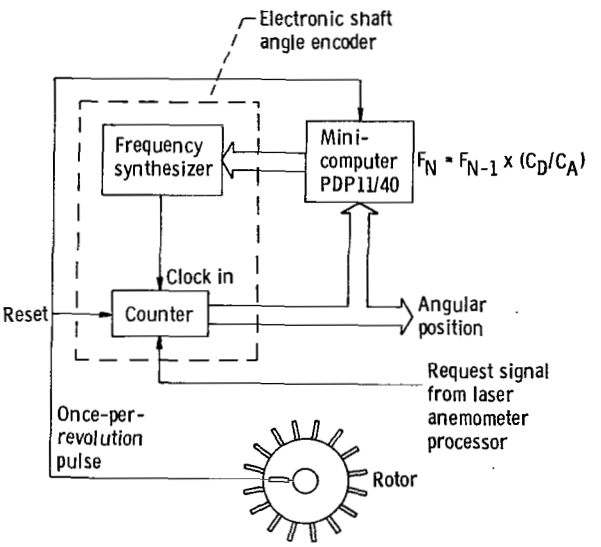

Figure 4. - Method for generating the rotor angular position.

counts for each revolution (selected by the operator) remains approximately constant. An optical sensor (fig. 5) generates the OPR pulse as a result of a passing target on the rotor hub. At this pulse the current count is read into the output buffer register of the counter, the counter is reset to zero, and the minicomputer is interrupted. The minicomputer then calculates a new synthesizer frequency using the equation

$$f_n = f_{n-1}\left(\frac{C_D}{C_A}\right)$$

where f_n is the new frequency, f_{n-1} is the frequency programmed on previous revolution, C_D is the desired count for one revolution, and C_A is the actual count for previous revolution. The synthesizer is then programmed with the new frequency. Thus, the number of counts for each revolution remains approximately constant, independent of rotor speed. The actual algorithm for calculating the updated synthesizer frequency is described in appendix A. At each velocity measurement a request signal causes the current count to be transferred to the output buffer register where it can be recorded with the velocity.

The synthesizer frequency is updated near the beginning of each revolution, so it is important that the updating process take place quickly with no loss in output clock pulses during the process. The synthesizer used in this system meets both these requirements, with a programming time of less than 0.4 microsecond.

This technique is capable of providing the angular position for very-high-speed turbomachines. The upper limit for the rotational speed can be expressed as

Maximum rotational speed (rpm) =

Maximum synth. frequency (Hz) × 60(sec/min)/C_D(counts/rev)

An operational requirement for this scheme is that the fractional change in the angular velocity of the rotor for each revolution be small compared to the desired resolution in the angular position expressed as a fractional part of one revolution. Otherwise, it would be necessary to adjust the synthesizer frequency more than once during each revolution in order to adequately track the rotor speed. This requirement was easily met in the research facility to which the anemometer was applied. For example, the 52-bladed research rotor was operated at speeds up to about 16 000 rpm. The desired count was chosen to be 200 counts per blade passage for a total count per revolution of 10 400. The long term (i.e., 1 sec) speed drift in the facility was about 0.3 percent (30 counts out of 10 400), but the revolution-to-revolution speed changes were less than one count. For all results and examples cited in this paper, the encoder count was divided by four to yield a resolution of 50 angular positions (angles) per blade passage. However, this anemometer can be used with either 50, 100, or 200 angles per blade passage.

Description of System Software

General Comments

Increasingly, as instruments are being applied to more difficult and/or complex experiments, computers and

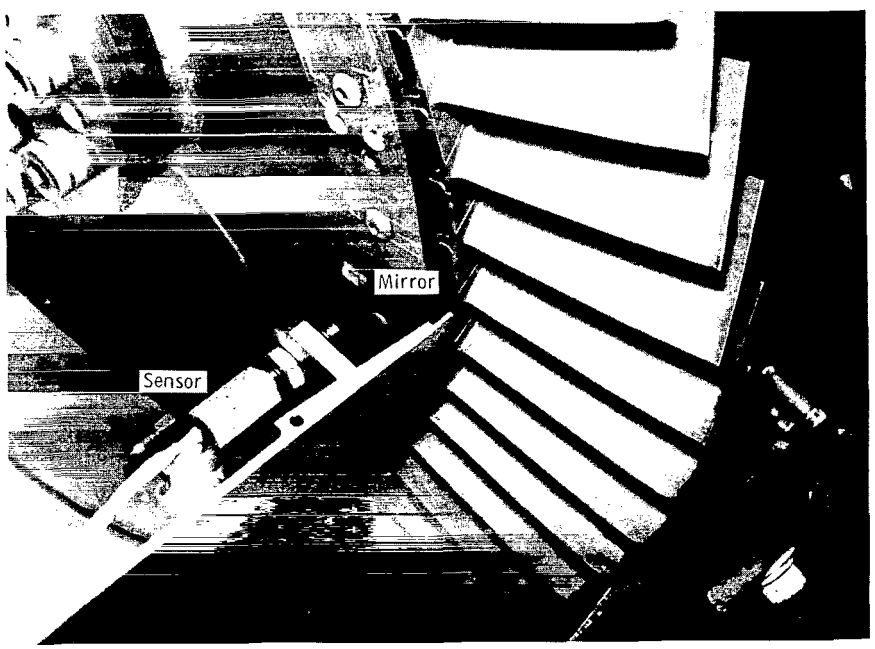

Figure 5. - Photograph of the once-per-revolution optical sensor and target mirror on rotor hub.

their associated software are assuming a larger proportion of the development time. In the anemometer being described, more than half of the development time was spent on the software. Among the software design goals was the use of a high-level language (e.g., Fortran) in those cases where operating speed is not important.

Figure 6 shows a block diagram of the measurement program for determining velocity profiles. The upper four modules are in Fortran. Because of execution speed requirements, the lower three routines are in assembly language. Flow charts for these three routines are given in appendix B. After the required parameters are initialized and appropriate tables are cleared, the main program determines the routing to the various subroutines. The following sections describe the functions of these subroutines.

Once-per-revolution (OPR)

There are two routines that are called in response to a hardware interrupt signal, and the higher priority of the two is the OPR routine. Its primary function is to service the electronic shaft angle encoder. At the OPR pulse this routine causes the current shaft encoder count to be read, calculates the new synthesizer frequency, and then updates the synthesizer. If the current encoder count is not within some preset tolerance of the desired count, typically 0.1 percent, then the velocity data accumulated in the previous revolution is discarded. This prevents velocity data from being assigned to the wrong angular position if the encoder is not properly tracking the rotor speed. Improper tracking could be caused by changing flow conditions or electronic noise on the once-per-revolution signal. The OPR routine requires about 200 microseconds, which is about 5 percent of a revolution at 16 000 rpm. Hence, this fraction of the circumferential path is not available for velocity measurements.

Data Acquisition

This is the other interrupt routine. Its function is to respond to the anemometer's counter-type processor. When a validated measurement has been obtained by the LA processor, a "data ready" signal interrupts the minicomputer, which then reads both the transit time and the corresponding angular position (angle). If the angle is one of the 1000 angles being accepted, the data are put into one of two temporary buffers for further processing (fig. 7). If the angle is beyond the range of those angles being accepted, the routine is disabled until the next OPR occurrence. This allows data in the buffers to be processed for the rest of the revolution without interruption. This routine, the shortest of all the routines in execution time, requires about 40 microseconds. It essentially sets a limit on the rate at which velocity data can be accumulated.

Data Processing

This routine processes the data that have been placed in the temporary buffers. At any given time one of the buffers is being loaded with data and the other is being emptied as the data are processed. The reason for the two buffers is that, as mentioned previously, after each revolution the total encoder count is compared with the desired count. If the count is within some preset tolerance and if the buffer being emptied is empty, then the roles of the two buffers are exchanged; that is, the buffer being emptied in the previous revolution will now be the buffer being loaded with new data. This exchange is done in the OPR routine. However, if a spurious OPR pulse was detected during the previous revolution, the encoder may have inserted incorrect position data into the buffer being loaded. An indication of this problem will show up in the OPR routine where the total count will not be within tolerance. In this case the data in the buffer being loaded in the previous revolution will be discarded.

An important consideration in the use of the minicomputer was the amount of available random access memory, in this case, the core memory. Recording all transit time-angle data pairs would quickly fill the available memory. For example, 30 000 measurements

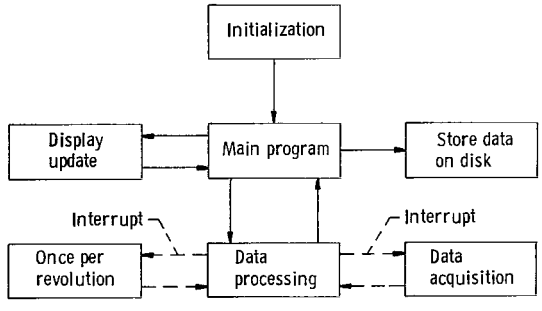

Figure 6. - Diagram of minicomputer routines used in anemometer measurement program.

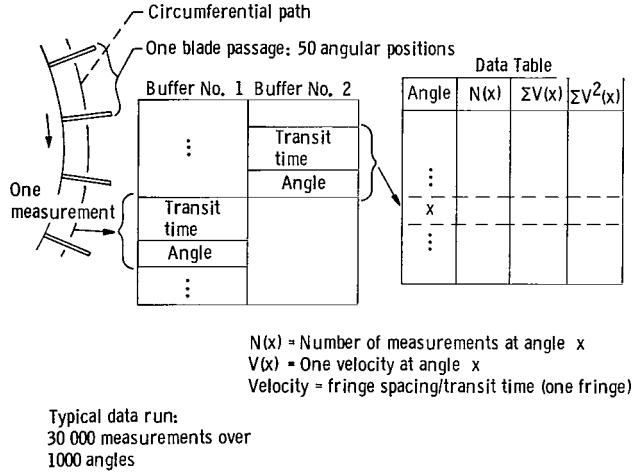

Figure 7. - Data acquisition and processing scheme.

would require 60 000 words of storage, but there are only about 10 000 words available for storage. Also, the data would not be in a form that could easily be converted into a real-time display. To reduce the amount of storage required, the approach taken in recording data is shown in figure 7. At each rotor angular position (i.e., angle x), the following information is stored: (1) the number of measurements at each angle, $N(x)$; (2) the sum of the velocities, $\Sigma V(x)$; and (3) the sum of the velocities, squared, $\Sigma V2(x)$. With this information, the mean velocity and standard deviation can be calculated for every angle.

To obtain the velocity from the processor data output, a number of data processing steps are taken. The processor output is actually a time measurement (transit time) in a special floating-point format (mantissa exponent). The transit time is first transformed into an integer representation of the velocity. Since the velocity is inversely proportional to the transit time, this step involves taking the reciprocal of the transit time. In integer form the velocity is used in the comparison test described below. The velocity is then converted to the two-word, floating-point format compatible with a real variable in Fortran. In this format the quantities, $\Sigma V(x)$ and $\Sigma V2(x)$ are calculated. The quantity $N(x)$ is a one-word integer. The data table thus consists of five 16-bit words, $N(x)$, $\Sigma V(x)$, and $\Sigma V2(x)$, for each angle. For 1000 angles the data table takes up 5000 words of storage. The magnitude of the angle defines the location of the five words within the table.

A data run, consisting of two parts, is completed for each probe volume position and beam orientation. This enables an additional method for discarding bad data. There is concern for bad measurements, since there are only an average of 30 measurements per position and a single bad measurement can significantly affect the result. In the first part of the data run velocity data from corresponding positions from all 20 blade passages are combined to form an averaged velocity, $\overline{V}(J)$, where $J=1$ to 50, for each position in the averaged blade passage. In this paper we shall refer to this averaged blade passage as the ensemble-averaged blade passage. This can be expressed as

$$\overline{V}(J) = 1/20 \sum_{I=1}^{20} V[J+50(I-1)] \qquad J=1 \text{ to } 50$$

where

$\overline{V}(J)$ velocity at the Jth position within the ensemble-averaged blade passage

J angle position index within the ensemble-averaged blade passage, $J=1$ to 50

I blade-passage index, $I=1$ to 20

As discussed in the next section these averages are used in the real-time display.

In the second part of the data run, each measured velocity value is compared with the corresponding previously obtained average. If the difference is more than 25 percent, that value is rejected as bad data. A total of 30 000 measurements are made and recorded for each part of every data run.

The data processing routine continues between interrupts until (1) the desired number of measurements has been obtained, or (2) it is time for a display update. In either case control returns to the main program. If the desired number of measurements has been obtained, a routine is called that transfers the data table to a magnetic disk.

Display Update

To be able to evaluate data being accumulated, a routine to provide a real-time graphic display on the CRT was developed. An example of this display is shown in figure 8. The display is normally updated every 15 seconds, but the time between updates can be set to any value greater than 5 seconds. The display consists of three parts. The upper part is an alphanumeric presentation of some of the operating conditions. For example, it includes the elapsed time (in seconds) since the beginning of a data run to obtain a velocity profile. The remainder of the alphanumerics are discussed in the Results section.

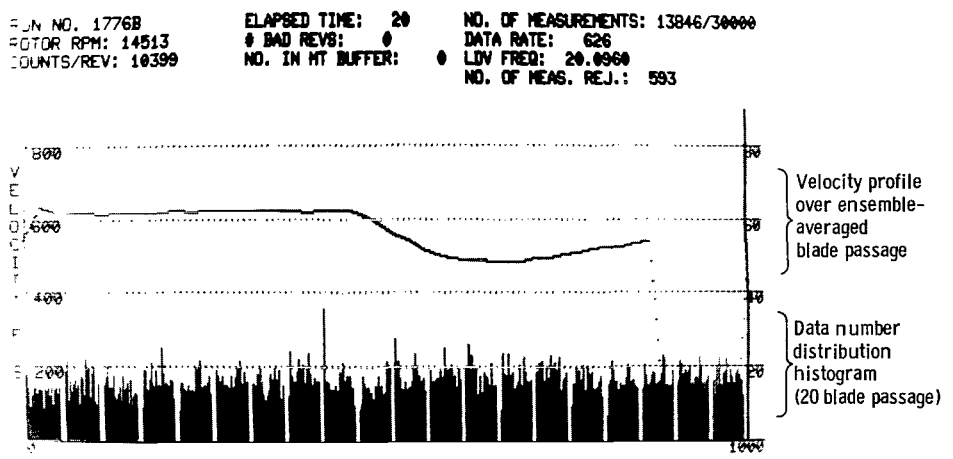

Figure 8. - CRT real-time presentation of accumulated data.

The lower part is a histogram of the number of measurements over the 1000 angles covering the 20 blade passages ($N(x)$, where $x=1$ to 1000). The abcissa ranges from 0 to 1000, and the ordinate ($N(x)$, listed on the right side of the histogram) ranges from 0 to 80 measurements.

The middle part is a plot of the velocity profile ($\overline{V(J)}, J=1$ to 50) over an ensemble-averaged blade passage. The abcissa ranges over a circumferential segment with a length of one blade pitch. Note that the abcissa for the velocity profile covers only one blade passage, while the abcissa for the histogram covers 20 blade passages. The ordinate (listed on the left side) is in feet per second. It is obtained by ensemble-averaging velocity data from each of the 20 blade passages.

When a CRT update is required, data acquisition is suspended for about 1 second while the necessary graphic information is calculated. The transmission of the graphic information to the CRT terminal is interspersed with the data processing routine (see appendix B), so the 3-second time for transmission has only a small effect on the overall measurement rate.

Optics Position Control

When the optics needs to be reset, the minicomputer transmits a set of new motor positions to the microcomputer. The microcomputer then calculates the direction and number of pulses each motor must receive to reach the new position. The correct pulse trains are then transmitted in parallel to the corresponding motor drives. If the number of pulses returned by the encoder on each motor shaft agrees with the number of pulses transmitted to each motor, the optics are assumed to be at position and ready for measurements. The microcomputer then transmits an "at position" signal to the minicomputer and measurements resume. If the numbers do not agree, an error message is transmitted to the minicomputer and appropriate action taken. The software for the minicomputer for this operation is written in Fortran, except where assembly language is required in the transmission of data. The software for the microcomputer is written in PL/M language (ref. 13) except for the transmission of pulses to the motor drives.

The equations that relate motor positions to the desired measurement positions and velocity component relative to the rotor are given in appendix C. These equations are complicated by the various degrees of freedom that have been built into the position optics.

Additional Software

A blade-geometry program was developed that performs a number of functions relative to probe volume position and input-beam direction. One function is to generate a CRT graphic display showing the position of the circumferential measurement line relative to the rotor blades. A sample CRT display is shown in figure 9 where three different views of the rotor blades are presented. In this display the blade cross-sections are generated from the blade-contour coordinates obtained from the mechanical specifications for the rotor being tested. The selected cross-sectional planes are those planes that contain the points of intersection of the measurement line with the rotor blade. (The numbers shown in fig. 9 are various position coordinates. They will not be discussed in this paper.)

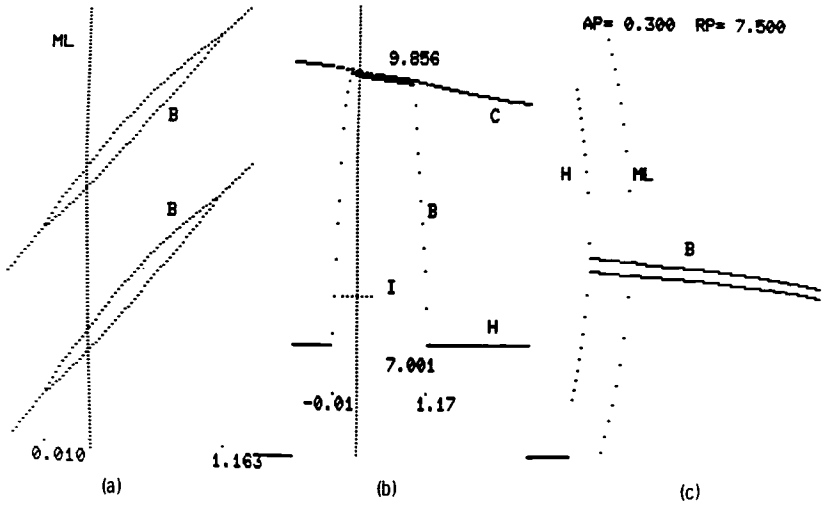

B rotor blade cross section
C casing
H rotor hub
I intersection of measurement line with plane of paper
ML circumferential measurement line

Figure 9. - CRT presentation of three views of circumferential measurement line relative to the rotor blades. (a) View along a radius. (b) View perpendicular to rotation axis. (c) View along a line parallel to the rotation axis.

A second function of the blade-geometry program is to calculate the optimum input-beam direction. This need arises because the curved and twisted rotor blades cause partial optical blockage (or, shadowing) of the blade passage. The program generates another CRT display showing an enlarged cross-sectional view of the curved blade and the optical blockage for any given input-beam direction. A sample of this display is shown in figure 10. At the optimum input-beam direction the shadowing is minimized.

Finally, a third function of the blade-geometry program is to calculate a starting rotor angle so that velocity measurements always begin on the suction side of a blade. The starting angle will vary with both probe volume position and input-beam direction. This latter function contributes to a more useful real-time graphic display of the velocity profile.

The LA measurement program was written so that a number of operating options are presented to the user at the beginning of a series of measurements. The options include the starting rotor angle for velocity measurements, the total number of measurements, and the time between CRT display updates.

During operation the LA measurement program and the optics position control program are chained together; that is, after a velocity profile is obtained, the optics are automatically positioned for the next profile. Normally, at a given axial and radial probe volume position, two velocity-component measurements are taken under the same flow conditions. The beam-bisector direction is the same for both of these velocity-component measurements. The velocity-component and flow angle in a plane perpendicular to the beam-bisector direction is then calculated. The two velocity components are automatically taken 30° apart. The choice of 30° is a compromise based on several considerations. The absolute flow angle can vary 20° to 30° over a velocity profile. To obtain good resolution in the measured velocity magnitude and flow angle, the two velocity-component directions should span the expected directions. However, if the span is too great, statistical angle biasing errors may occur (ref. 11).

Other computer programs were written so that the acquired velocity data can be analyzed in detail immediately with the minicomputer. For example, combining the absolute velocity magnitude and flow angle with the rotor speed can yield velocities relative to the moving rotor blades. Figure 11 is a sample CRT display of such a relative velocity profile for an ensemble-averaged blade passage. Numerous other quantities can be calculated and presented in either tabular or graphical form. These quantities can be presented on the CRT for each of the 20 blade passages, or for an ensemble-averaged passage.

System Performance

Experimental Procedure

The initial application for the anemometer was in a single-stage transonic compressor research facility. The first test rotor had 52 blades, an inlet tip diameter of 50.8 centimeters, and a hub-tip radius ratio of 0.7. The 100-percent design tip speed for the rotor was 426 meters per second, corresponding to a rotor speed of 16 000 rpm.

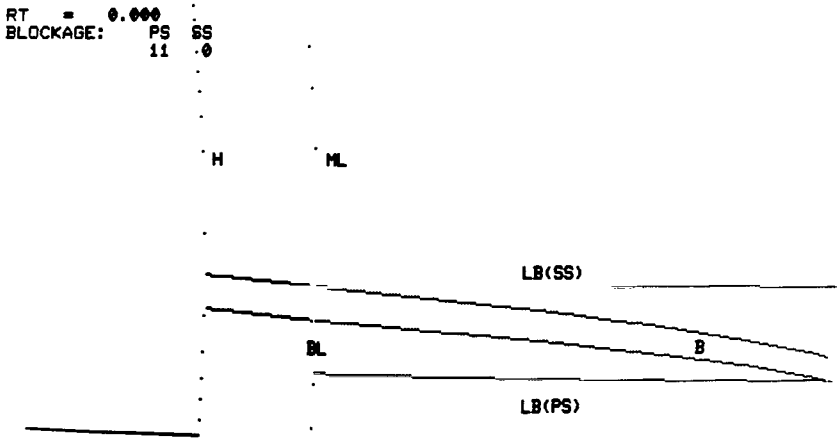

B rotor blade cross section
BL portion of measured line that is blocked
H rotor hub
LB laser beams
ML circumferential measurement line
PS pressure side of blade
SS suction side of blade

Figure 10. - CRT graphics display that shows the optical blockage of the measurement line by the rotor blade. In this example, blockage is on the pressure side of blade. This is a view looking along a line parallel to the rotation axis.

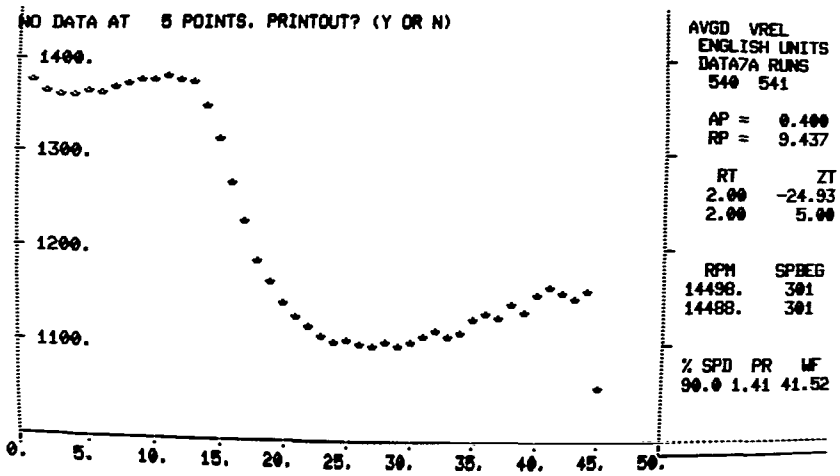

Figure 11. - CRT display of plot of flow velocity relative to the rotor (in ft/sec) for an ensemble-averaged blade passage. Two velocity profiles taken at the same flow conditions were combined to produce this plot.

Optical access to the rotor was made along a nominally radial path through a window in the casing. The window was ordinary double-strength window glass (3 mm thick) that was contoured to match the inside wall of the casing. The contouring was accomplished by allowing the glass to sag onto a machined graphite form in a vacuum furnace. The window, which was not optically coated, had a clear aperture of 5.1 centimeters along a circumference and 10.2 centimeters in the axial direction.

When the probe volume is near a solid surface, scattered laser light from the surface tends to dominate the collected signal. As a result, this interfers with measurements made near the casing window and the rotor hub. To minimize this problem, the fluorescent dye technique (ref. 14) was used. In this technique fluorescent seed particles absorb the laser light and then emit light at a different wavelength. An optical filter in the receiving optics filters out the unwanted laser light scattered from surfaces near the probe volume. The selected seed material was a 0.02 molar solution of rhodamine 6G in a 50-50 mixture (by volume) of ethylene glycol and benzyl alcohol. This particle material fluoresces orange when it absorbs the green laser light. Thus, when the orange-pass filter is placed in the receiving optics, the extraneous green scattered light is filtered out. A commercial atomizer produced the seed particle aerosol by feeding the liquid into a high velocity jet (located within the atomizer). The mean diameter of the particles that were actually measured was estimated to be about 1.2 to 1.4 micrometers. This estimate is based on (1) particle lag in crossing shocks within the rotor and (2) separate experiments involving particle acceleration through a nozzle with known flow conditions.

The use of the fluorescent dye in the seed particles allowed measurements to within 1 millimeter of the rotor hub and casing window. As the probe volume approached the hub or window surface (within 1 mm), the data rate decreased to zero. This is reasonable since the probe volume is 2 millimeters long. Without the fluorescent dye, measurements could not be made closer than 10 millimeters from these surfaces.

During operation the window and rotor gradually became coated with oil and the fluorescent dye. This reduced the signal-to-noise ratio and the data rate. So about once an hour, the window was washed with a solution that was nothing more than standard automotive windshield-washing fluid. The procedure was to pump the fluid to a line of small holes just upstream of the rotor with the rotor speed reduced to about 10 000 rpm. The sheeting action of the fluid over the window was very effective in cleaning the window.

Results

Velocity measurements were taken over operating conditions ranging from 50 to 100 percent of design speed. A detailed description and discussion of the results are given elsewhere (ref. 10). However, sufficient description is given here to illustrate the capabilities of the anemometer.

The encoder worked very well in providing the rotor angular position information. For example, at 16 000 rpm the average deviation of the actual encoder count from the desired count for a complete revolution was about 3 counts out of 10 400 (200×52 blades). Remembering that each rotor angular position is obtained by dividing the encoder count by four, the average error in the angular position at the end of a revolution was 0.75 of the angular position increment used. As the rotor speed drifts up and down, the position error generally is a minimum at the beginning of a revolution when the synthesizer update occurs and a maximum at the end. The 20 blade passages selected for measurements were normally in the first half of each revolution. Thus, the actual average error in the rotor angular position was about 0.4 of an angular position increment out of the 50 position increments used for each blade passage.

Velocity profiles along circumferential paths covering 20 consecutive blade passages (i.e., 50 angular positions per blade passage × 20 blade passages) were determined and recorded. Typically, the profiles consisting of 30 000 measurements over 1000 angular positions were obtained in 15 to 45 seconds. Axial and radial positions that were mapped included the region upstream and downstream of the rotor as well as within the blade row. At 90 to 100 percent, design speeds shocks were measured in front of and within the blade row.

The real-time display shown in figure 8 is a typical result and was obtained at 90 percent of design speed (14 513 rpm) within the blade row. It shows that ensemble-averaged velocity profile for one blade passage at 20 seconds into the second part of a data run where 13 846 out of a requested 30 000 measurements have been obtained. The data rate of 626 per second is only approximate since the time of 20 seconds is only approximate. The LDV FREQ of 20.096 megahertz is a typical value of the LA frequency calculated from the LA processor output. A total of 593 measurements have been rejected because they differed by more than 25 percent from the corresponding average obtained in the first part of the data run. The COUNTS/REV of 10 399 is a typical value of the encoder count for one rotor revolution. In this case the desired count was 10 400. The BAD REVS is the number of revolutions since the beginning of part two of the data run where the total encoder count for one revolution differed from the desired count by more than the preset tolerance (in this case, 10). The NO. IN MT BUFFER is the number of transit time-angle data pairs in the temporary data buffer being processed. If this number becomes large, it indicates the minicomputer is not keeping up with the data being collected. The knee of the velocity profile is where a shock occurs. The gap at the right is where the blade occurs for the ensemble-averaged blade passage. The gaps in the histogram at the bottom are where the 20 individual blades occur. At the edge of the eighth gap from the left there is a spike in the number of measurements. This is probably caused by this particular blade becoming coated with the fluorescent dye.

The accuracy of measurements made with a fringe-type anemometer is strongly dependent on each application. Pertinent factors include the flow conditions, signal-to-noise ratio of each signal burst, system noise, etc. In a laboratory calibration of the anemometer against a circular jet with known flow characteristics, velocities measured with the anemometer agreed with the calculated flow to within 1 percent. It was concluded that systematic errors were less than 1 percent. In the application to the axial compressor rotor, an error analysis (ref. 10) indicated that the random errors were such that the velocity profiles determined for the ensemble-averaged blade passage are accurate to within about 3 to 5 percent of reading (for a 95 percent confidence level).

Concluding Remarks

This paper has described an anemometer that was designed to make intrarotor flow measurements in turbomachinery rapidly and efficiently. Another design goal was to maximize the size of the intrarotor region that is mapped. The application of the anemometer to a transonic axial compressor rotor demonstrated that these goals were met. Detailed measurements of shocks and intrarotor flow velocities have been obtained. The scheme whereby velocities are accepted from many different angular positions at any given time works very well. Velocity profiles along a circumferential path covering up to 20 blade passages can be determined, typically, in about 30 seconds. An added benefit of this scheme is the high spatial resolution along the resulting velocity profile.

The real-time display developed for the anemometer is helpful in achieving efficient operation. As an example, both the ensemble-averaged velocity profile and the histogram are useful indicators of extraneous velocity data due to light scattering by the rotating blades. When this problem is significant, corrective action can be taken (e.g., input laser beam direction can be changed).

The capability of changing the input laser-beam direction allows a decrease in the portion of the intrarotor region that is optically blocked by the curved and twisted rotor blades. By operating at a calculated optimum input direction, this blade shadowing is minimized.

Lewis Research Center
National Aeronautics and Space Administration
Cleveland, Ohio, March 17, 1981

Appendix A – Synthesizer Frequency Update

The software for calculating a new synthesizer frequency for each rotor revolution uses integer arithmetic to minimize the time required for the calculation. The limitations of the 16-bit minicomputer requires a particular sequence of steps to implement the arithmetic. These calculations are contained in the once-per-revolution assembly language interrupt routine.

The minicomputer is capable of (1) adding two 32-bit integers, (2) multiplying two 16-bit integers to get a 32-bit product, and (3) dividing a 32-bit integer by a 16-bit integer to get a 16-bit quotient and a 16-bit remainder. The example given in the section on the shaft angle encoder illustrates the minicomputer limitations. In this example, a 52-bladed rotor is operated at speeds of 16 000 rpm with a desired angular position resolution of 200 counts per blade passage. These numbers yield 10 400 counts per revolution and a synthesizer frequency of 2.773 megahertz.

The obvious methods of calculating the updated synthesizer frequency (f_n) are

$$f_n = f_{n-1}\left(\frac{C_D}{C_A}\right) \quad \text{or} \quad f_n = \frac{(f_{n-1} \times C_D)}{C_A}$$

$$\text{or} \quad f_n = \left(\frac{f_{n-1}}{C_A}\right) C_D$$

where f_n and f_{n-1} are 32-bit integers, and C_D (desired count) and C_A (actual count) are 16-bit integers. The quotients (C_D/C_A) and (f_{n-1}/C_A) are truncated to form integers. The first method will not work, since (C_D/C_A) does not yield a useful integer. In the second method $f_{n-1}C_D$ can exceed 32 bits. Using the above example to illustrate the third method, an error (due to decreasing rotor speed) of 25 counts ($C_A = 10\,425$) would be required before the integer derived from (f_{n-1}/C_A) would change. So, this method also is not very useful.

A more useful (and equivalent) form of the above equation is

$$f_n = f_{n-1} + \left(\frac{f_{n-1}}{C_A}\right)(C_D - C_A)$$

With this expression, the sequence of calculations is this: (1) determine the count error ($C_D - C_A$) for the previous revolution; (2) calculate the actual rotational speed (f_{n-1}/C_A)(in this case, the resolution will be sufficient); (3) calculate the change required in the previous frequency, (f_{n-1}/C_A)($C_D - C_A$); and (4) add the required frequency change to the previous frequency.

The frequency synthesizer is then updated by outputting the two 16-bit words that represent f_n. The frequency synthesizer used in this system has a programming delay of less than 0.4 microsecond following the update signal and loses no output pulses during the programming process. This synthesizer capability allows velocity measurements to be made every revolution, even though the synthesizer is updated near the beginning of every revolution.

Appendix B – Flow Charts

The flow charts in this appendix show the logical sequence of events during the once-per-revolution (fig. 12) and data acquisition (fig. 13) interrupt routines and the data processing routine (fig. 14). These are the time-critical routines so they are written in assembly language.

The information for the CRT display update is contained in a table of 8-bit characters. As can be seen in figure 14, these characters are transmitted to the CRT, one character at a time, in the data processing routine. With this procedure the slow transmission rate to the CRT does not significantly slow down the measurement process.

The major time-consuming parts of the data processing routine (fig. 14) are the floating-point arithmetic steps. However, without the hardware floating-point capability, the minicomputer would take much longer to perform these calculations.

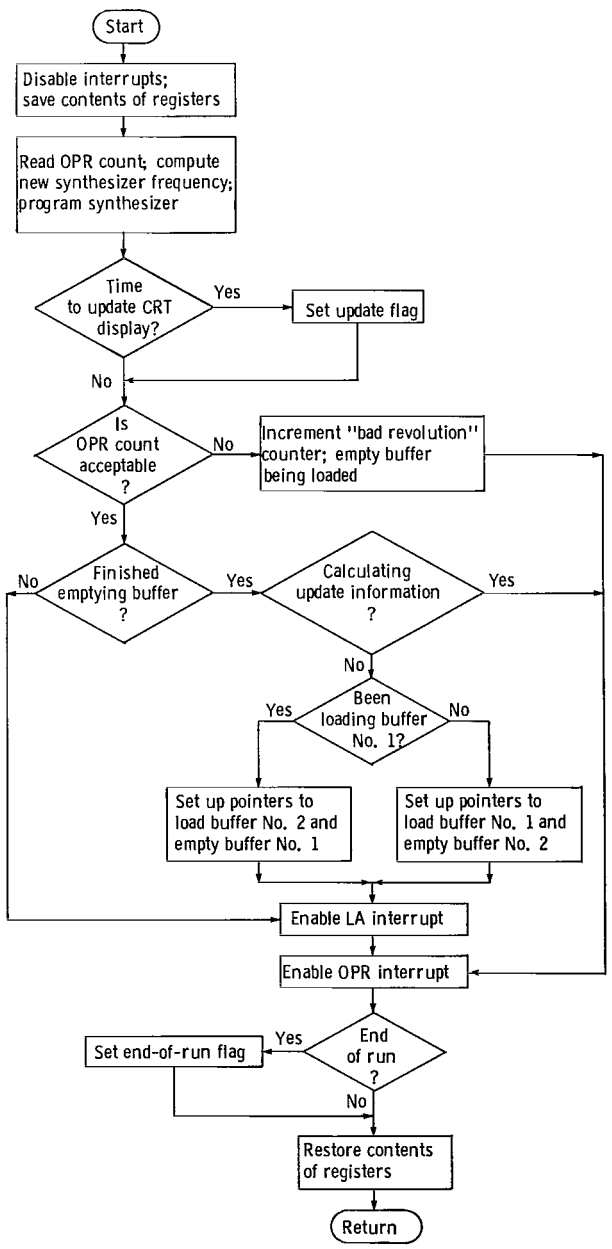

Figure 12. - Flow chart for the once-per-revolution (OPR) interrupt routine.

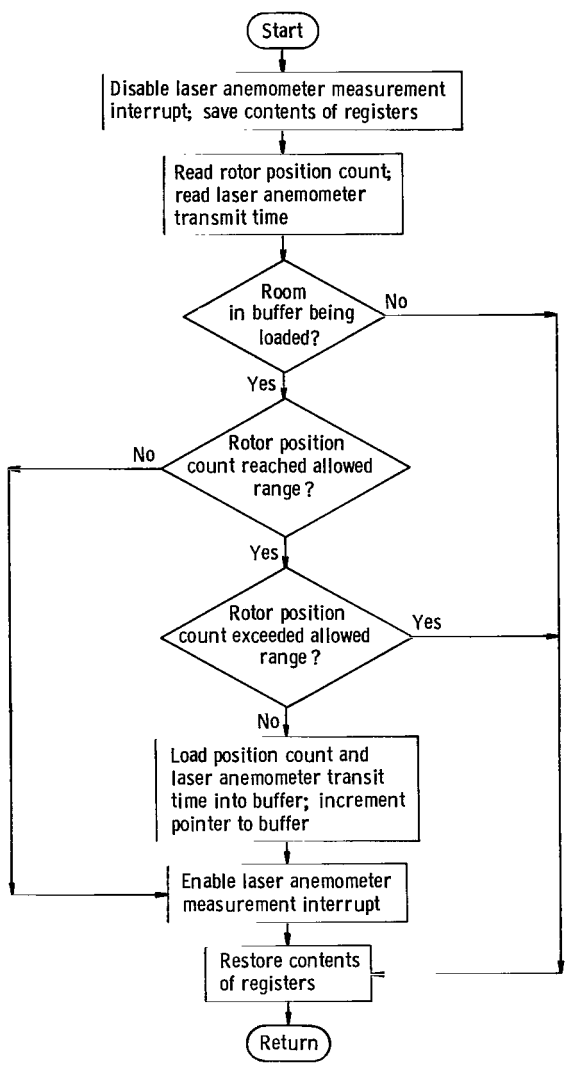

Figure 13. - Flow chart for data acquisition interrupt routine.

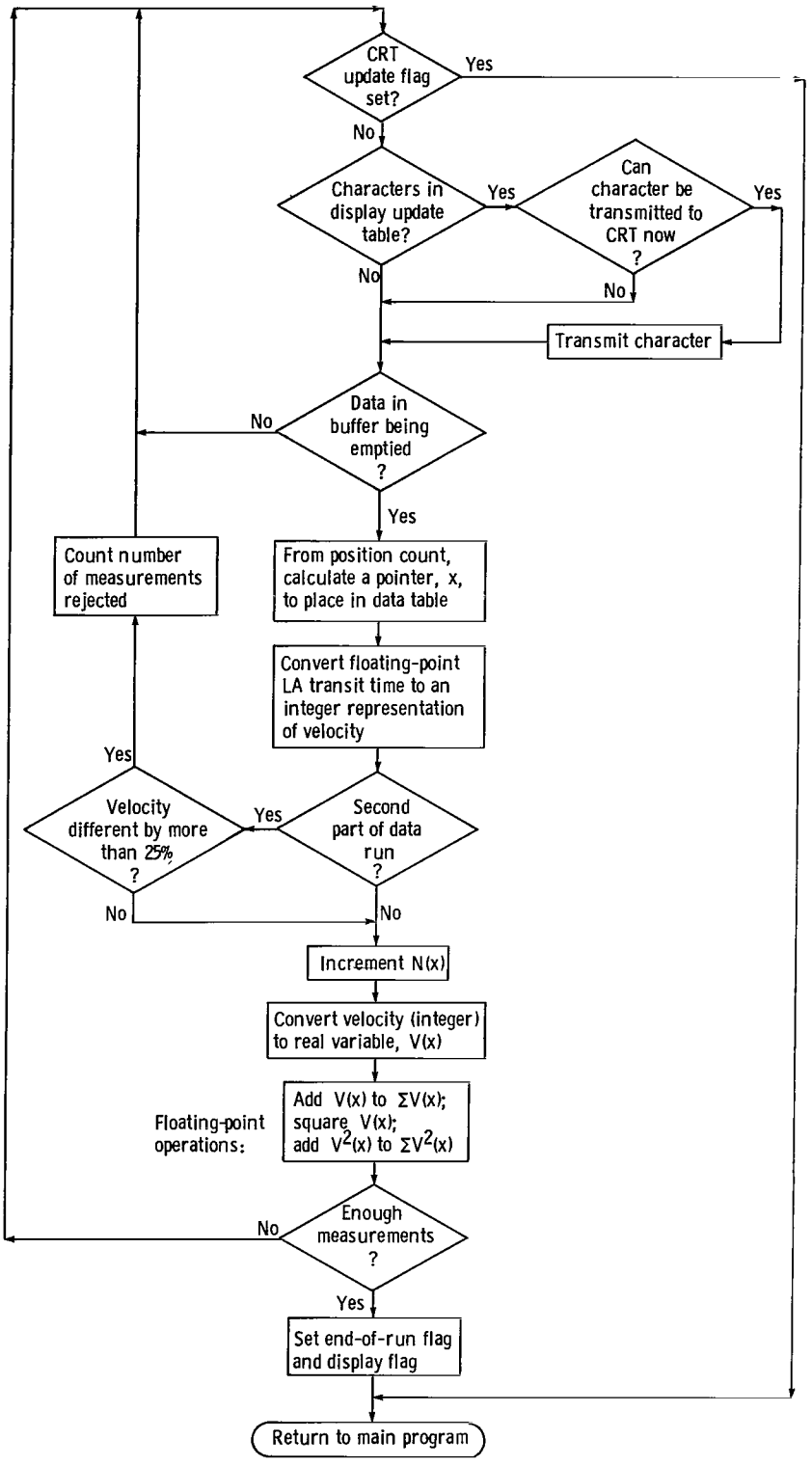

Figure 14. - Flow chart for the data processing routine.

Appendix C – Optical-Component Position Coordinates

Determining the probe volume position and velocity-component direction relative to the rotor for each velocity measurement is complicated by the various degrees of freedom for the optical components, and, of course, the rotor rotation. A major complicating factor is the ability to change input laser-beam direction relative to the radial direction. In this appendix equations are given that express the probe volume position (and the velocity component being measured) in several different frames of reference. These equations allow the calculation of stepping motor positions corresponding to a user-defined set of position coordinates.

As described previously, four stepping motors are used to position the optical components, shown in figure 1. The complete optics package is mounted on an x-y positioner that is driven by two of the motors. This allows the probe volume to be positioned axially and radially. A third motor rotates the beam splitter (selects the velocity component) and the fourth moves the goniometer (changes input beam direction).

The goniometer can be moved such that the bisector to the two input laser beams remains in a vertical plane perpendicular to the axis of rotor rotation. When the goniometer mirror moves this bisector from the horizontal plane (i.e., when it is no longer along a radius to the rotor rotation axis), there are three effects to consider. First, the probe volume will be on a different circumferential measurement line. Second, a different velocity component will be measured. And third, the probe volume position along the circumferential line will be affected.

For convenience and flexibility of software, the four coordinates describing the optical-component positions were defined in the following three frames of reference.

(1) User-specified frame of reference. The user normally specifies the position coordinates in this frame (figs. 15 and 16). There are two right-handed Cartesian coordinate systems, RZY and R′ZY′. The Z-axis is parallel to the rotor rotation axis and is in the direction of the flow. The R-axis is along a radius from this rotation axis and is in a horizontal plane. The RZY coordinate system is fixed relative to the laboratory frame, and the R′ZY′ system is fixed relative to the goniometer mirror. Note that the two coordinate systems coincide when the goniometer mirror is vertical.

RP radius of the circumferential measurement line relative to the rotor rotation axis (fig. 16).

AP axial position of the measurement line (relative to the rotor-blade leading edge at the intersection with the hub). This coordinate is not shown in the figure.

ZT velocity-component angle defined to be equal to the angle between the normal to the fringe plane and the Z-axis. This normal is parallel to the Z-Y′ plane and is in the direction of the velocity component being measured.

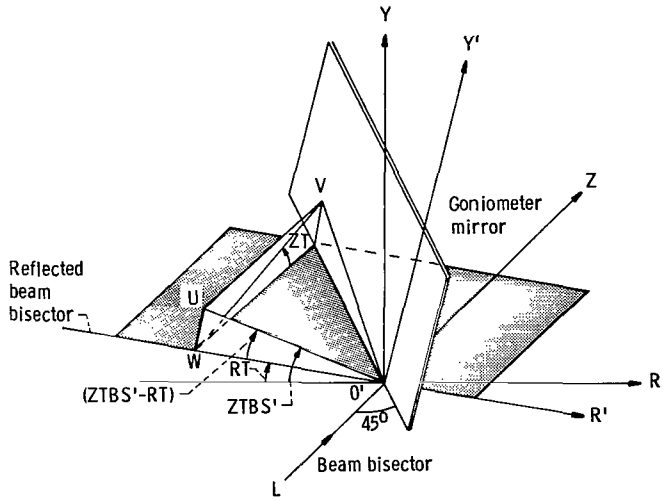

(a) Goniometer mirror.

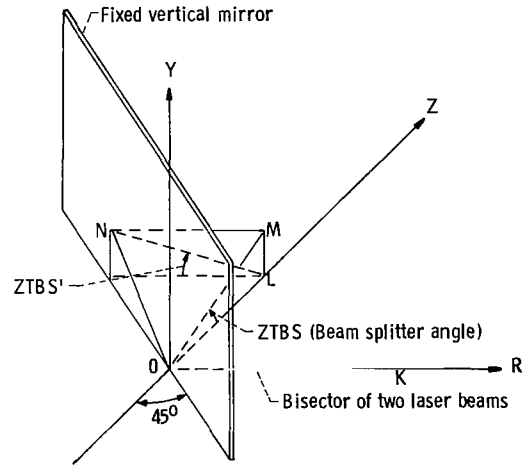

(b) Fixed vertical mirror.

Figure 15. - Effect of two mirrors on rotation about bisector of two laser beams.

RT angle of tilt of the goniometer mirror (i.e., the angle of R′ relative to R). The user specifies this angle to minimize shadowing of the opics by the curved rotor blades.

Note that RP, AP are linear coordinates, and ZT, RT are angular coordinates.

(2) Relative frame of reference. In this frame the position of each of the four motor-drive axes is expressed relative to the rotor axis. The coordinates AP and RT are the same as for the user-specified frame.

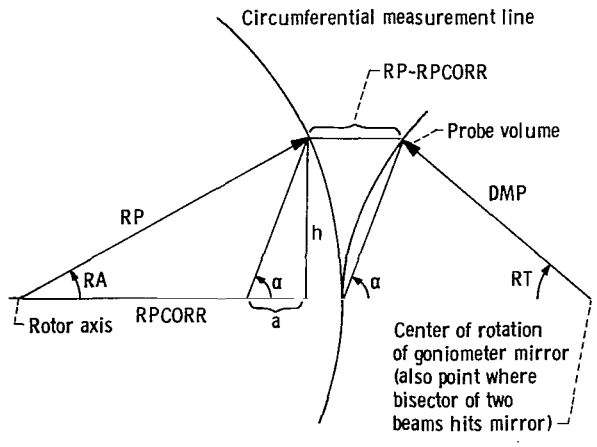

Figure 16. - Diagram showing effect of tilting goniometer mirror on probe volume position.

RPCORR distance from rotor rotation axis at which probe volume circle (the circle of radius DMP in fig. 16) intersects motor drive axis, such that, with a goniometer mirror tilt angle RT, the probe volume lies on the circumferential measurement line with radius RP.

ZTBS beam splitter angle measured relative to the horizontal plane in a counterclockwise direction looking along the beam direction. Refer to figure 15(b). The two laser beams will lie in the ONM plane when the beam splitter angle is ZTBS. Also note that the beam bisector lies along the R-axis.

Note that the optical table must be moved a distance RP-RPCORR in order that the probe volume will fall on the circumferential measurement line.

(3) Absolute frame of reference. In this frame the position of each motor-drive axis is expressed relative to its home position.

The relationship between the beam splitter angle (ZTBS) and the actual velocity-component angle (ZT) will now be determined. Keep in mind that the velocity-component direction is normal to the bisector of the two beams (at the probe volume). At any point in the optical path, the beam bisector can be thought of as a line equidistant between the two beams and in the plane of the beams. It is sufficient to follow the beams bisector through the optics and to determine what happens to a rotation about this bisector. There are two optical components to consider: the fixed vertical mirror just after the two beams emerge from the beam splitter and the goniometer mirror (see fig. 1).

The effect of the fixed vertical mirror is shown in figure 15(b). This mirror is at a 45° angle to the R and Z axes of the RZY coordinate system. In this figure the origin of the coordinate system is positioned at the point where the beam bisector hits the vertical mirror. Before reflection the two beams lie in the plane ONM. After reflection the two beams lie in the plane ONL, and the beam bisector lies along the Z-axis. Because this is a reflection from a plane mirror, the angle ZTBS′ equals the angle ZTBS (the beam splitter angle). However, the sense of rotation is reversed.

Figure 15(a) is used to show the relationship between ZTBS′ and ZT. The origin of the two coordinate systems are positioned where the beam bisector hits the goniometer mirror. Before reflection the two beams lie in the plane O′UV. Note that plane O′UV coincides with plane ONL. After reflection, the two beams lie in the plane O′WV, and the beam bisector lies along the R′-axis (in the negative direction). Again, because this is a reflection from a plane mirror, the angle ZTBS′-RT is equal to the angle ZT. From the above arguments, we can write

$$ZT = ZTBS - RT$$

The relationship between RP and RPCORR can be determined in the following way. In figure 16 DMP is defined to be the distance of the probe volume from the point where the beam bisector strikes the goniometer mirror. This distance (DMP) remains unchanged and is measured experimentally. From the geometry of the figure, it can be shown that

$$RA = \sin^{-1}\left[\frac{DMP\ \sin(RT)}{RP}\right] \quad \text{and}$$

$$RPCORR = RP\ \cos(RA) - DMP[1 - \cos(RT)]$$

For computing RP from RPCORR it can be shown that

$$a = 2\ DMP\ \sin^2(RT/2)$$

$$h = DMP\ \sin(RT) \quad \text{and}$$

$$RP = \sqrt{(RPCORR + a)^2 + h^2}$$

Note that RP = RPCORR when RT = 0.

The user specified position corrdinates (RP, AP, ZT, and RT) are first converted to the relative frame of reference (RPCORR, AP, ZTBS, and RT) and then to the absolute frame. This second conversion is required since the motor drives are referenced to a "home" position relative to each motor drive axis. This latter conversion also includes a change from a user-chosen set of units (e.g., millimeters, degrees, etc.) to motor steps. A general equation for this second conversion can be expressed as

$$ABPOS - ABREF = \pm(\text{scale factor}) \times (RELPOS - RELREF)$$

where

ABPOS motor position corresponding to a position coordinate expressed in the absolute frame of reference (i.e., referenced to the motor drive "home" position)

ABREF motor position that corresponds to some convenient calibrated position expressed in the absolute frame of reference

RELPOS motor position corresponding to the above position coordinate, but expressed in the relative frame of reference

RELREF motor position that corresponds to the above calibrated position expressed in the relative frame of reference

The scale factor converts the user set of units in the relative frame to motor steps in the absolute frame. If the absolute and relative frames of reference are in the same direction, the positive sign is used in the above equation. If not, the negative sign is used.

As mentioned, the third effect of rotating the goniometer mirror is that the probe volume position along the circumferential line is changed. When a velocity measurement is made, the angle encoder outputs an angular position relative to a target on the rotor rub. This relative angular position is calibrated with the probe volume in the horizontal plane containing the rotation axis. Thus, when the angle RT is not zero, the angular position of the probe volume must be corrected by the angle RA (see fig. 16).

References

1. Durst, F.; Melling, A.; and Whitelaw, J. H.: Principles and Practice of Laser Doppler Anemometry. Academic Press, 1976.
2. Wisler, D. C.; and Mossey, P. W.: Gas Velocity Measurements Within a Compressor Rotor Passage Using the Laser Doppler Velocimeter. J. Eng. Power, vol. 95, no. 2, Apr. 1973, pp. 91–96. (ASME Paper 72-WA/GT-2, Nov. 1972.)
3. Wisler, D. C.: Shock Wave and Flow Velocity Measurements in a High Speed Fan Rotor Using the Laser Velocimeter. J. Eng. Power, vol. 99, no. 2, Apr. 1977, pp. 181–188. (ASME Paper 76-GT-49, Mar. 1976).
4. Schodl, R.: Laser Dual-Beam Method for Flow Measurements in Turbomachines. ASME Paper 74-GT-157, Mar. 1974.
5. Eckardt, D.: Detailed Flow Investigations Within a High-Speed Centrifugal Compressor Impeller. J. Fluids Eng., vol. 98, no. 3, Sep. 1976, pp. 390–402. (ASME Paper 76-FE-13, Mar. 1976.)
6. Dunker, R. J.; Strinning, P. E.; and Weyer, H. B.: Experimental Study of the Flow Field Within a Transonic Axial Compressor Rotor by Laser Velocimetry and Comparison with Through-Flow Calculations. J. Eng. Power, vol. 100, no. 2, Apr. 1978, pp. 279–286. (ASME Paper 77-GT-28, Mar. 1977.)
7. Caspersen, C.: A Special Data-Processing Method for LDA Signals from Flow Near and Between Rotating Components. Measurement Methods in Rotating Components of Turbomachinery, B. Lakshminarayana and P. Runstadler, Jr., eds., American Society of Mechanical Engineers, 1980, pp. 111–118.
8. Schodl, R.: A Laser-Two-Focus (L2F) Velocimeter for Automatic Flow Vector Measurements in the Rotating Components of Turbomachines. Measurement Methods in Rotating Components of Turbomachinery, B. Lakshminarayana and P. Runstadler, Jr., eds., American Society of Mechanical Engineers, 1980, pp. 139–147.
9. Powell, J. A.; Strazisar, A. J.; and Seasholtz, R. G.: Efficient Laser Anemometer for Intra-rotor Flow Mapping in Turbomachinery. Measurement Methods in Rotating Components of Turbomachinery, B. Lakshminarayana and P. Runstadler, Jr., eds., American Society of Mechanical Engineers, 1980, pp. 157–164.
10. Strazisar, A. J.; and Powell, J. A.: Laser Anemometer Measurements in a Transonic Axial Flow Compressor Rotor. Measurement Methods in Rotating Components of Turbomachinery, B. Lakshminarayana and P. Runstadler, Jr., eds., American Society of Mechanical Engineers, 1980, pp. 165–176.
11. Seasholtz, R. G.: Laser Doppler Velocimeter System for Turbine Stator Cascade Studies and Analysis of Statistical Biasing Errors. NASA TN D-8297, 1977.
12. Owners Manual, 2096, 2098 LV Processors. Macrodyne, Incorporated, Schenectady, New York, Sep. 1976.
13. 8008 and 8080 PL/M Programming Manual. Intel Corporation, Santa Clara, Calif., 1975.
14. Stevenson, W. H.; dos Santos, R.; and Mettler, S. C.: Fringe Mode Fluorescence Velocimetry. Applications of Non-Intrusive Instrumentation in Fluid Flow Research, AGARD CP-193, 1976, pp. 20-1 to 20-9.

Lewis motion-picture film supplement C-292 is available on loan. Requests will be filled in the order received.

The film (16 mm, 14 min, color, sound) explains and then shows the operation of the laser anemometer described in this report in Lewis' single-stage transonic compressor facility. A real-time graphic display of an actual data run is presented. Additional graphic displays showing blade geometry and a review of velocity data are included.

Requests for film supplement C-292 should to be addressed to:

NASA Lewis Research Center
Attn: Chief, Management Services Division (5-5)
21000 Brookpark Road
Cleveland, OH 44135

cut

Date _____

Please send, on loan, copy of film supplement C-292 to TP 1663

Name of Organization

Street Number

City and State Zip Code

Attention: Mr.

Title

1. Report No.	2. Government Accession No.	3. Recipient's Catalog No.
NASA TP-1663		

4. Title and Subtitle	5. Report Date
HIGH-SPEED LASER ANEMOMETER SYSTEM FOR INTRAROTOR FLOW MAPPING IN TURBOMACHINERY	February 1982
	6. Performing Organization Code: 505-32-82

7. Author(s)	8. Performing Organization Report No.
J. Anthony Powell, Anthony J. Strazisar, and Richard G. Seasholtz	E-276
	10. Work Unit No.

9. Performing Organization Name and Address	11. Contract or Grant No.
National Aeronautics and Space Administration Lewis Research Center Cleveland, Ohio 44135	

12. Sponsoring Agency Name and Address	13. Type of Report and Period Covered
National Aeronautics and Space Administration Washington, D.C. 20546	Technical Paper
	14. Sponsoring Agency Code

15. Supplementary Notes

16. Abstract

Innovative features of the anemometer include (1) a rapid and efficient data acquisition process, (2) a detailed real-time graphic display of the data being accumulated, and (3) input laser-beam positioning that allows greater optical access to the intrarotor region. Results are presented that demonstrate the anemometer's capability in flow mapping within a transonic axial-flow compressor rotor. Typically, a velocity profile, derived from 30 000 measurements along 1000 sequential circumferential positions covering 20 blade passages, can be obtained in 30 seconds. The use of fluorescent seed particles allows flow measurements near the rotor hub and the casing window. A film supplement illustrating the operation of the anemometer is available.

17. Key Words (Suggested by Author(s))	18. Distribution Statement
Laser anemometer Turbomachinery	Unclassified - unlimited STAR Category 35

19. Security Classif. (of this report)	20. Security Classif. (of this page)	21. No. of Pages	22. Price*
Unclassified	Unclassified	20	A02

* For sale by the National Technical Information Service, Springfield, Virginia 22161

NASA-Langley, 1982

National Aeronautics and Space Administration

Washington, D.C.
20546

Official Business
Penalty for Private Use, $300

THIRD-CLASS BULK RATE

Postage and Fees Paid
National Aeronautics and
Space Administration
NASA-451

U.S.MAIL

3 1 1U,D, 022382 S00903DS
DEPT OF THE AIR FORCE
AF WEAPONS LABORATORY
ATTN: TECHNICAL LIBRARY (SUL)
KIRTLAND AFB NM 87117

NASA

POSTMASTER: If Undeliverable (Section 158 Postal Manual) Do Not Return